

Photocatalytic degradation of rhodamine B by nano bismuth oxide: Process modeling by response surface methodology (RSM)

Seyed Ali Hosseini*, Ramin Saeedi

Department of Applied Chemistry, Urmia University, 5756151818, Urmia, Iran.

Received 27 April 2016; received in revised form 18 October 2016; accepted 1 November 2016

ABSTRACT

The photocatalytic activity of nano-Bi₂O₃ was evaluated in degradation of rhodamine B (RhB) as a model of dye pollutant from waste waters. Nano sized Bi₂O₃ was synthesized using the chemical precipitation method. The as-prepared sample was characterized by X-ray diffraction (XRD), scanning electron microscopy (SEM) and Fourier transform infrared spectrometry (FT-IR). Structural analysis revealed that Bi₂O₃ contains a unique well-crystallized phase and the average crystallite size of 22.4 nm. The SEM analysis revealed that the size of Bi₂O₃ particles was mainly in the range of 16-22 nm. Response surface methodology was applied to design experiments and to optimize the photocatalytic process. A second order model was developed and a good correlation was found between experimental and predicted responses, confirming the reliability of the model. The optimal condition for maximum degradation of values of RhB resulted in initial concentration, irradiation time, initial pH and catalyst dosage of 12.5 mg.L⁻¹, 120 min, 4.6-7 and 0.75 g.L⁻¹, respectively. The Bi₂O₃ nanoparticles exhibited an efficient ultraviolet photocatalytic activity so that under optimal condition more than 95% of Rhodamine B was decolorized. The Pareto analysis indicated that the order of relative importance of the input variables on the dye degradation efficiency is as follows: Bi₂O₃ dosage > pH ≈ irradiation time > initial concentration of the RhB.

Keywords: Nanoparticle, Bismuth nano oxide, photocatalytic dye degradation, Response surface methodology, Pareto analysis.

1. Introduction

Due to printing and dyeing industries, their wastewater as one of the industrial wastewaters is hard to treat because of its higher concentration, deep chromes, great toxicity and complicated component [1]. In particular, the pollution of water resources by organic pollutants, such as phenolic compounds, various dyes, etc. threatened the health of human beings [2]. Applications of the existing conventional physical-chemical and biological techniques represent unsatisfactory outcomes because of ineffective or nondestructive mineralization of these recalcitrant compounds [3]. Photocatalytic degradation of organic pollutants, such as RhB, a typical stable dyestuff, has proved to be a viable, environmentally benign technology to the discoloration and degradation of dye effluents [4]. In this method, electrons and holes will form by illuminating a semiconductor with a UV or Vis radiation with a suitable energy.

These electron-holes pairs, in turn, produce free radicals to decompose a large number of organic effluents [5]. In particular, nano-sized semiconductor particles with suitable surface areas and a variety of morphologies offer great opportunity [5]. Titanium dioxide (TiO₂) is one of the most effective photocatalysts because it is biologically and chemically inert [7]. Nevertheless, because of its large band gap of 3.2 eV, the TiO₂ needs UV light irradiation to produce the electronic transition responsible to its photo activity [8]. Bi₂O₃ is an important metal oxide semiconductor with a direct band gap ranging from 2 to 3.9 eV and can be used to decompose dyes in water under UV and visible light irradiation. Furthermore, Bi₂O₃ is rather inert in neutral water, which is a fundamental precondition for applications of a photocatalyst for wastewater purification [9]. Bi₂O₃ has been prepared by solid-state reaction, sonochemical route, thermolysis, or hydrothermal treatment. The photo degradation of Rhodamine B, methyl orange, and peroxomonosulfate has been observed in the presence of Bi₂O₃ monoclinic [10]. For example, Qin et al.

*Corresponding author email: a.hosseini@urmia.ac.ir
Tel: +98 44 3194 2026; Fax: +98 44 3275 5294

prepared Bi_2O_3 and $(\text{BiO})_2\text{CO}_3$ Nanotubes by a solvothermal method and evaluated their activities by photocatalytic degradation of RhB and CrVI-removal [11]. Pan et al. synthesized Bismuth Oxide Nanoparticles by a Templating method and tested its photocatalytic performance by decolorization of methyl orange solution under visible light condition [12]. The efficiency of a photocatalytic reaction depends on a number of factors, which govern the performance of photocatalysis. Initial concentration of pollutant, photocatalyst concentration, pH, volume of solution, radiant flux and agitation, irradiation time, light intensity, irradiation wavelength, temperature, geometrical parameters of the experimental setup and multiple degradation pathways are the parameters that can be cited. Due to the complexity and variety of influencing factors, it is difficult to evaluate the relative significance of several affecting factors, especially in the presence of complex interactions [13]. The aim of this work is to optimize the conditions of photocatalytic degradation of Rhodamine B with Bi_2O_3 nano-oxide by applying the response surface methodology (RSM). Different variables, namely, the amount of catalyst, initial pH, irradiation time, and initial dye concentration are considered for optimization.

2. Experimental

Bismuth nitrate pentahydrate, sodium hydroxide, hydrochloric acid, nitric acid and Rhodamine B all were purchased from Merck chemicals. All materials were used without further purification. The nano- Bi_2O_3 was synthesized by the precipitation method. First, a bismuth solution (0.2 mol.L^{-1}) was prepared by dissolving 9.70 g of $\text{Bi}(\text{NO}_3)_3 \cdot 5\text{H}_2\text{O}$ in 0.1L nitric acid (1.50 mol.L^{-1}). Then, 60.20 mL of concentrated sodium hydroxide (2.50 mol.L^{-1}) was added drop by drop to the above-mentioned solution until pH reached 11.5. The white precipitate was appeared immediately and after several hours turned to yellow one. It was kept under magnetic stirring at room temperature for 24 h [10]. The collected precipitates were filtered, washed several times with distilled water and dried in an electric oven at $50 \text{ }^\circ\text{C}$ for 5 h. The structure and phase characteristic of as-prepared Bi_2O_3 was determined by X-ray diffraction patterns [XRD, Philips Xpert diffractometer using $\text{Cu K}\alpha$ radiation]. The data were recorded in the $4\text{-}60^\circ$ 2θ range with 0.02° steps. The morphology of the sample, coated with gold, was examined using scanning electron microscopy Tescan (Mira 3). The absorption data of degraded aqueous solutions were collected using a UV-Vis spectrometer. Photocatalytic activity of Bi_2O_3 was measured by

degradation of RhB under UV irradiation. As UV-C irradiation, a 15 W UV lamp (Philips, Netherlands) was used. For each experiment, a certain amount of the catalyst, based on design of experiments (DOE), was suspended in 100 mL dye solution. Prior to illumination, the suspension was stirred continuously in the dark for 30 min to ensure the establishment of an adsorption between dye and surface of the catalyst. Then, the pH was adjusted using NaOH and HCl (0.10 mol.L^{-1}). Next, the solution was illuminated according to DOE. At the given intervals, 3 mL aliquots were taken out and centrifuged to remove the catalysts. The samples were analyzed by UV-Vis spectroscopy. The degradation percentage D , was calculated with Eq.1.

$$D\% = \frac{A_0 - A_t}{A_0} \times 100 \quad (1)$$

Where A_0 and A_t are the initial and final absorbance of dye, respectively.

2.1. Determination of the point of zero charge

The point of zero charge of the Bismuth nano-oxide was determined using the mass titration (MT) method suggested by Subramanian and coworkers [14]. Several aqueous suspensions containing various amounts of the immersed Bi_2O_3 and 10 ml of NaCl (0.1M) as electrolyte were prepared and agitated for 24 h in a shaker at 220 rpm to reach an equilibrium pH values. Then, the curve pH versus sorbent mass was plotted. The plateau in the MT curve corresponds to pH_{pzc} .

2.2. Response surface methodology (RSM)

Response surface methodology (RSM) is a family of statistical techniques for the design, empirical modeling and optimization of processes, where the responses of interest are influenced by several process variables (termed factors). RSM comprises the following three major components: (i) experimental design to determine the values of process factors based on which experiments are conducted and data are collected; (ii) empirical modeling to approximate the relationship (i.e., the response surface) between responses and factors; (iii) optimization to find the best response value based on the empirical model. In addition, the above three-stage procedure is typically operated in an iterative manner, where the information attained from previous iterations is utilized to guide the search for better response variables. RSM is particularly applicable to problems where the understanding of the process mechanism is limited and/or is difficult to be represented by the first-principles mathematical model. Depending on specific objectives in practice, these RSM techniques differ in

the experimental design procedure, the choice of empirical models, and the mathematical formulation of the optimization problem [15]. In the present work, Box-Behnken design (BBD) was used for the optimization of photocatalytic degradation of RhB by nano-Bi₂O₃. The use of Box-Behnken design is popular in industrial research because it is an economical design and requires only three levels (-1, 0, 1) for each factor [16]. The most important factors, which affect the photocatalytic degradation of dye effluents in aqueous solution are the catalyst amount, initial concentration of dye, initial pH and irradiation time. Therefore, the effect of the above four factors on the photocatalytic degradation of RhB was studied as the independent, process-specific variables and degradation percentage as a response. The four independent variables were converted to dimensionless ones (X₁, X₂, X₃, X₄), with the coded values at levels: -1, 0, +1. Values and limits of independent variables, determined by preliminary experiments, are shown in Table 1. A total of 27 experiments for RhB degradation consisting of three-factorial and three BBD levels were applied in the present work, including one replication at the center point. The complete experimental design matrix and the responses based on experimental runs proposed by BBD for the photocatalytic degradation of RhB are given in Table 2. In the optimization process, BBD results were used for figuring, where Y is the selected response (dependent variable), X₁ to X_i are the independent variables being optimized. The calculation was aimed at predicting the better combination of independent variables for the optimization of the RhB photocatalytic degradation conditions. Accordingly, the best combination of X₁ (amount of catalyst), X₂ (initial pH), X₃ (irradiation time), and X₄ (initial dye concentration) for maximizing RhB degradation were achieved by using the below second-order polynomial equation 2.

$$Y = b_0 + \sum_{i=1}^n b_i X_i + \sum_{i=1}^n b_{ii} X_i^2 + \sum_{i=1}^{n-1} \sum_{j=i+1}^n b_{ij} X_i X_j \quad (2)$$

Where Y presents the predicted response, b_0 is the constant coefficient, b_i the linear coefficients, b_{ij} the interaction coefficients, b_{ii} the quadratic coefficients and X_i , X_j are the coded levels of the factors investigated. The coefficients of determination, R² and R²adj expressed fit quality of the resultant polynomial model, and statistical significance was checked by the F-test in the program. The desired goals in optimization were selected as maximum degradation of dye effluent (RhB) at a minimum catalyst amount, irradiation time, optimum initial pH, and maximum initial RhB concentration.

3. Results and discussion

3.1. XRD of nano-Bi₂O₃

The phase analysis and structure of as-prepared Bi₂O₃ was investigated using XRD pattern and the results are presented in Fig. 1. The strong diffraction peaks reveal high crystallinity of as-synthesized sample. All peaks are indexed to Bi₂O₃ with a monoclinic structure without any other impurity (JCPDS file No. 71-2274). The average crystalline size of 22.4 nm was calculated using the Debye-Scherrer (Eq.3).

$$\bar{D} = 0.89\lambda / \beta \cos\theta \quad (3)$$

Where λ , β and θ denote the X-ray wavelength (1.54 Å), the full-width at maximum intensity of the diffraction line and the diffraction angle, respectively [17].

3.2. FT-IR spectrum of nano-Bi₂O₃

The functional groups on the Bi₂O₃ were analyzed by FTIR technique and the related FTIR spectrum are shown in Fig. 2. The broad peak at 3451 cm⁻¹ is related to stretching vibration of hydrogen-banded surface water molecules and hydroxyl groups. The peak at 1628 cm⁻¹ corresponds to the vibrating mode of residual hydroxyl groups. The band at 847 cm⁻¹ implies the vibration of Bi-O bonds and existence of α -Bi₂O₃. This analysis is consistent with the reported literature pattern [18,19].

Table 1. Independent variables and their levels for the Box-Behnken design used in the present study.

Variable	Symbol	Coded Levels		
		(-1)	0	(+1)
Catal. Amount	X1	0.075	0	0.15
Initial pH	X2	2	7	12
Irradiation time(min)	X3	60	0	120
Dye. Concentration	X4	5	12.5	20

Table 2. Experimental design matrix and responses based on experimental runs proposed by BBD design for RhB degradation.

Run	Independent Variables				Response
	X ₁ Catalyst amount	X ₂ pH	X ₃ Irradiation time	X ₄ Dye concentration	
1	0.000	7	120	12.5	3.02
2	0.000	2	60	12.5	3.40
3	0.150	7	0	12.5	10.59
4	0.000	7	60	20.0	1.30
5	0.075	7	60	12.5	59.20
6	0.075	12	120	12.5	16.00
7	0.150	2	60	12.5	90.72
8	0.075	2	0	12.5	9.35
9	0.075	7	60	12.5	59.65
10	0.150	7	60	20.0	73.00
11	0.075	2	60	20.0	91.30
12	0.075	12	0	12.5	0.78
13	0.075	7	120	5.0	95.18
14	0.075	7	0	5.0	7.77
15	0.150	7	60	5.0	90.45
16	0.075	7	120	20.0	74.76
17	0.000	7	60	5.0	4.00
18	0.075	7	60	12.5	59.53
19	0.000	12	60	12.5	5.43
20	0.075	2	120	12.5	90.24
21	0.075	7	0	20.0	7.31
22	0.075	12	60	5.0	15.00
23	0.075	12	60	20.0	4.00
24	0.075	2	60	5.0	97.00
25	0.000	7	0	12.5	1.59
26	0.150	12	60	12.5	6.90
27	0.150	7	120	12.5	91.84

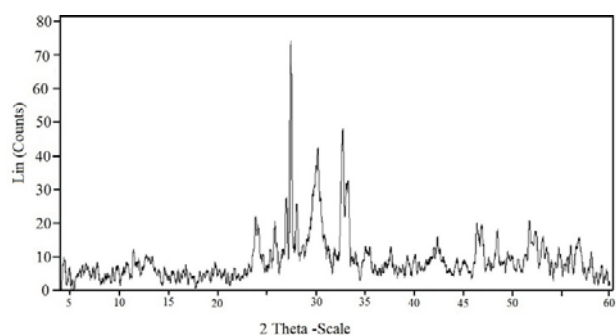


Fig. 1. XRD pattern of Bi₂O₃ nano oxide.

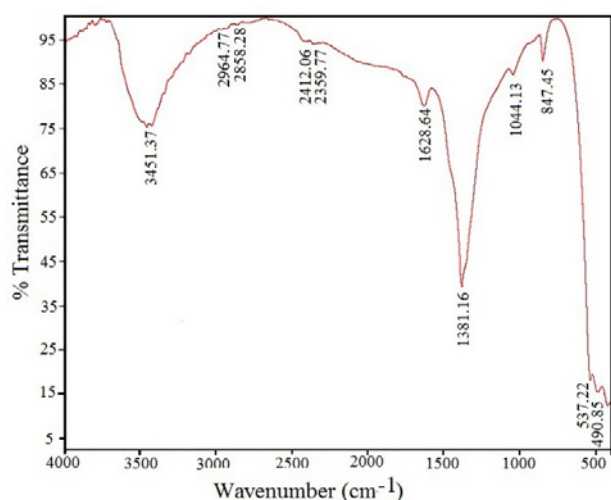


Fig. 2. FTIR spectrum of Bi₂O₃ nano oxide.

The morphology and particle size distribution of precursor was investigated by an emission-scanning electron microscopy. Fig. 3 shows SEM images of Bi₂O₃ prepared by the chemical precipitation method. SEM images indicate that the precursor predominantly consists of nearly spherical particles in the range 15.39-21.37 nm.

3.3. Data analysis and evaluation of the model by RSM

A semi-empirical model for the photocatalytic degradation of RhB was developed through data analysis by means of Minitab 16 software. Eq. 4 expressed the model in 12 statistically significant coefficients. Y is the degradation percentage of RhB.

$$Y = 62.38 + 28.73X_1 - 27.83X_2 + 27.80X_3 - 4.81X_4 - 20.17X_1^2 - 14.18X_2^2 - 16.89X_3^2 - 21.46X_1X_2 + 19.96X_1X_3 - 3.69X_1X_4 - 4.99X_3X_4 \quad (4)$$

Among the terms containing singular factor, the X₁ and X₃ have a positive synergistic effect on the response, whereas X₂ (pH) and X₄ (dye concentration) has an antagonistic effect on the response, meaning that an increase of dye concentration or solution pH decreases the removal percent of Rhodamine B.

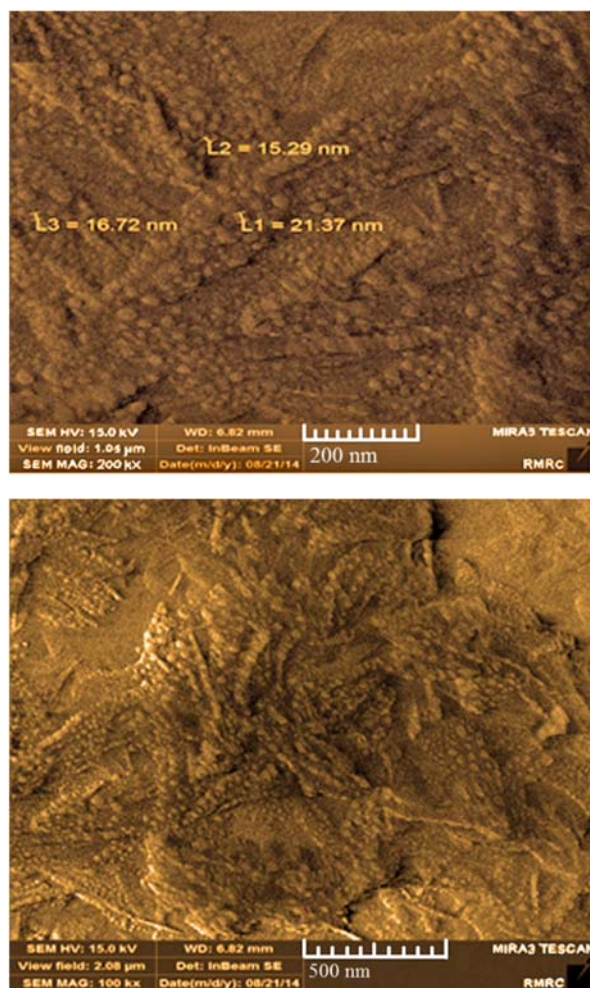


Fig. 3. SEM images of Bi₂O₃ nano oxide.

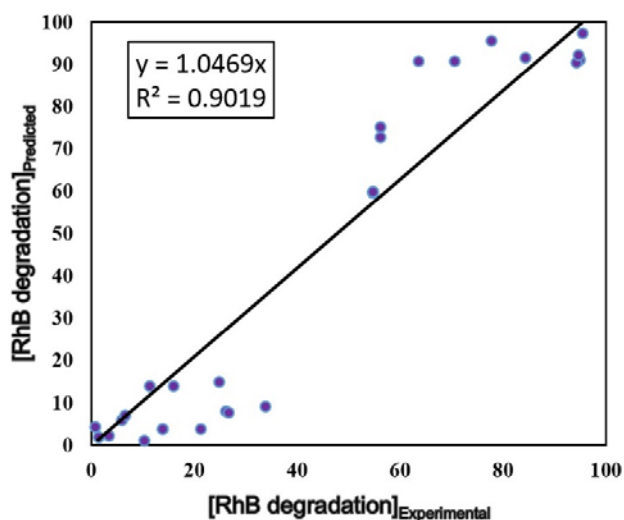
The results of analysis of variance (ANOVA) for the quadratic response surface model (Eq. 4) are presented in Table 3. ANOVA is a statistical technique that subdivides the total variation in a set of data into component parts associated with specific sources of variation for the purpose of testing hypotheses on the parameters of the model [20].

The Fisher's F-test was used to verify the statistical significance of the model. From the Fisher's F-test, the result shows that the established model is statistically significant (i.e., ratio of mean square regression to mean square residual) with F-value of 12.54. In addition, the significance of the model was evidenced by the determination coefficient (R²). The R² value means an acceptable agreement between the experimental and predicted values of the fitted data. Fig. 4 shows the plot of the predicted response by the model versus experimental responses and the R² value for them. A high correlation and high value of the determination coefficient (R²=0.9019) shows the validity of the model, revealing that the experimental values are in good agreement with the predicted values.

Table 3. Analysis of variance (ANOVA) for optimization of photocatalytic degradation of RhB.

Response	Source	Degrees of freedom	Sum of square	Mean square	F
RhB degradation	Regression	11	35984.0	3271.27	12.54
	Residual error	15	3913.7	260.91	
	total	26	39897.7		

$R^2 = 0.9019$, $R^2_{adj} = 0.83$

**Fig. 4.** Comparison between the experimental values of RhB degradation and those calculated by using the second-order polynomial Eq.(3) reported in the text (predicted values).

The adjusted R^2 (R^2_{adj}) = 0.83 is also of statistical significance and dictates the correlation applicability of the model. The P-values were used to check the significance of each coefficient of model terms, which, in turn, are necessary to understand the pattern of the mutual interactions between the test factors. The Student's t-test was used to determine the significance of the regression coefficient of the parameters, testing whether the true parameter is zero or not. P-value and t-value for each term of the model are presented in Table 4. Conventionally, the larger the t-value and the smaller the P-value ($p < 0.05$), the higher the significance of the corresponding coefficient will be. The coefficients of the linear effect of irradiation time, dye concentration, adsorbent dosage and pH with p-value of zero were significant. In the case of quadratic effects (X_i^2), all effects except the effects of X_2X_4 were significant at the confidence level of 95% and X_2X_4 was removed from the model. Moreover, the adequacy of the models was evaluated by the residuals (difference between the experimental and the predicted response value). The residuals can be considered as the variation unexplained by the fitted model and it is expected that they have a normal distribution [21].

Table 4. Estimated regression coefficient and corresponding t and p value.

Term	Coefficient	t-value	P-value
Constant	62.38	8.97	0.00
X_1	28.73	6.16	0.00
X_2	-27.83	-5.97	0.00
X_3	27.80	5.96	0.00
X_4	-4.81	-1.03	0.31
$X_1 * X_1$	-20.17	-3.06	0.00
$X_2 * X_2$	-14.18	-2.15	0.04
$X_3 * X_3$	-16.89	-2.56	0.02
$X_1 * X_2$	-21.46	-2.66	0.01
$X_1 * X_3$	19.96	2.47	0.026
$X_1 * X_4$	-3.69	-0.46	0.655
$X_3 * X_4$	-4.99	-0.62	0.54

The residuals can be considered as the variation unexplained by the fitted model and it is expected that they have a normal distribution [21]. Normal probability plots are a suitable graphical method for judging the normality of the residuals. The normal probability plot in Fig. 5a shows the values of predicted response against the residual values, given by a normal distribution. A graph of the residual versus the fitted value (predicted response) shows random behavior without a tendency towards residuals for experimental values (Fig. 5b). Fig. 5c shows the plot of residuals versus order of data, indicating randomly scattering and, consequently, the residual plots approve the adequacy of the model.

3.4. Standardized Pareto chart

Pareto analysis is applied to determine the relative importance of each term of the model. Pareto analysis calculates the percentage effect of each term on the response, according to equation 5 and gives some information to interpret the results.

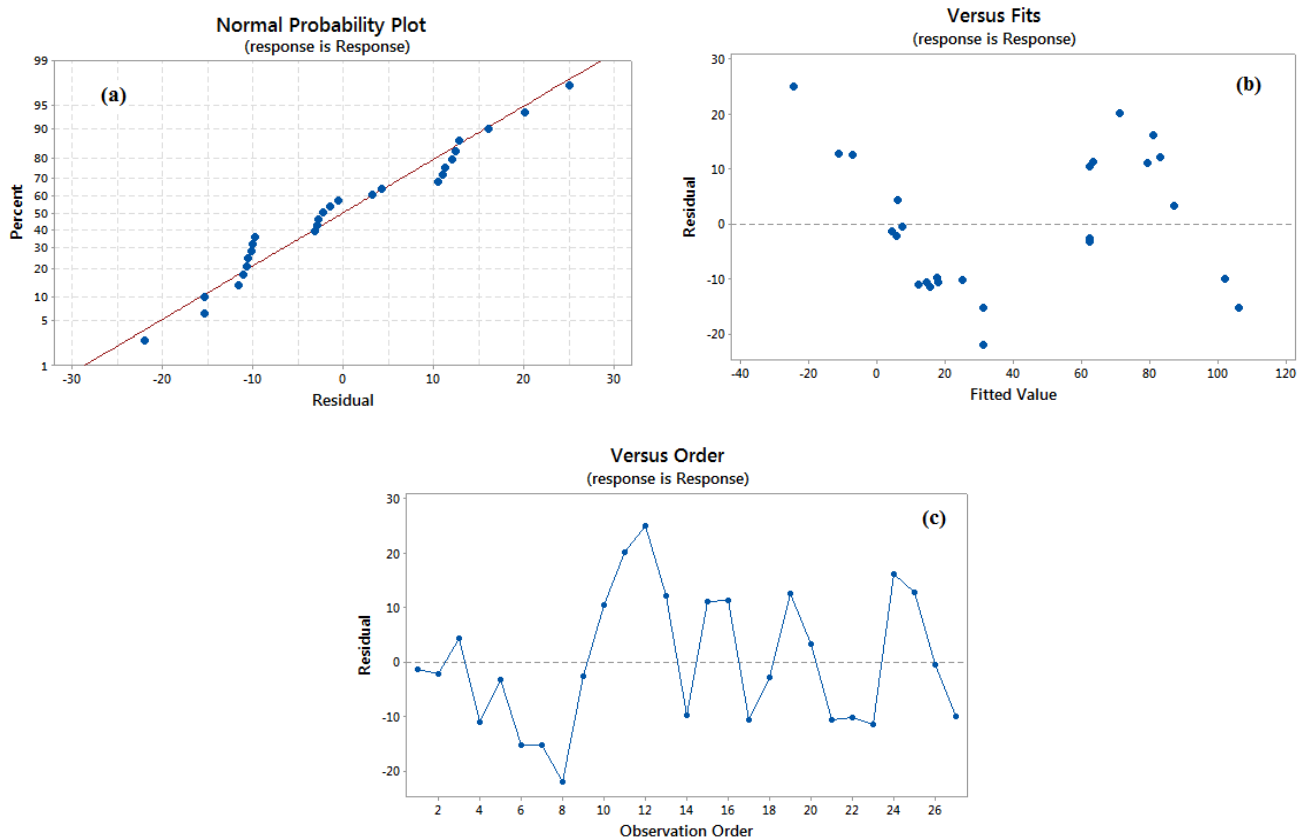


Fig. 5. Residual plots for predicted response by the model and experimental response.

$$P_i = \left(\frac{b_i^2}{\sum b_i^2} \right) \times 100 \quad (i \neq 0) \quad 3 \quad (5)$$

The results of Pareto analysis are shown in Fig. 6. The results suggest that the adsorbent dosage (X_4) with relative importance of 19.7% has the most important among the factors in the removal of the RhB. The Pareto analysis suggested that order of relative importance of the factors is as follows: X_1 (Adsorbent dosage) > X_2 (initial pH) \approx X_3 (irradiation time) > X_4 (dye concentration).

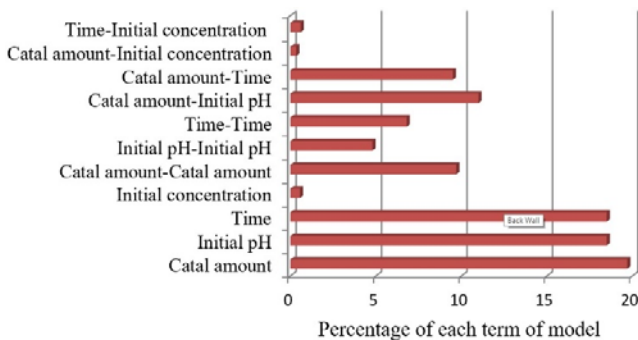


Fig. 6. Standardized effects of single and interaction factors on photocatalytic degradation of RhB.

3.5. Photocatalytic degradation of RhB

According to the above regression model equation and Pareto chart (Fig. 6), it was found that the adsorbent dosage and dye concentration have the maximum and minimum impacts on the response (RhB removal percent), respectively. Among binary terms, catalyst amount-pH (X_1X_2) and catalyst amount-irradiation time (X_1X_3) exhibited the highest impact on the response.

3.6. Effects of operational parameters on photocatalytic degradation process

The three-dimensional (3D) response surface plots as presented in Figs. 7a and 7b are graphical representations of the established regression equation (Eq. 4) to achieve better understanding of the interactions between factors and to determine the optimum level of each factor for maximum removal of RhB. The three-dimensional (3D) surface plots of the dependent factor (response of the model) as a function of two independent factors, maintaining all other factors at fixed levels can provide information on their relationships and can be helpful in understanding both the main and the interaction effects of these two independent factors. 2D contour plot is the projection of 3D surface plot on a two dimensional page.

Fig. 7a illustrates 3D surface plot and 2D contour plots for the combined interaction of adsorbent dosage and pH on the photocatalytic degradation of Rhodamine B.

From this Fig., it was found that pH has a negative impact when being coupled with adsorbent dosage (X_1). This was evidenced from the negative terms of X_1X_2 in Eq. (4) and also the convex response surfaces that indicate well-defined optimum variables. However, it must be emphasized that the singular catalyst dosage on its removal percentage has a positive impact as observed in Eq. (4). The catalyst dosage in photocatalytic processes is an important factor that can strongly influence the dye degradation [22]. According to Pareto analysis, the pH of RhB solution plays a prominent role on photocatalytic activity of Bi_2O_3 . In order to investigate the effect of pH on photodegradation of the RhB, several experiments according to DOE were done in three ranges: acidic (pH=2.0), neutral (pH=7.0) and basic (pH=12.0). The results showed that the degradation of RhB at pH=2 follows predominantly an adsorption process. The increase in the adsorption of Rhodamine-B with decreasing pH can be elucidated by considering the surface charge of the adsorbent materials. At low pH, neutralization of the negative charge at the surface of the adsorbents increases the protonation and results in higher adsorption of the dye on each adsorbent. This facilitates diffusion and results in a larger number of active sites on the surfaces of the adsorbents thereby enhancing adsorption at the surface [23]. The change of pH influences not only the molecular speciation of RhB in aqueous solution, but also the surface charge state of Bi_2O_3 . With the value of dissociation constant $pK_a = 3.7$ [24], the speciation of RhB in solution at different pH value changes. The RhB molecule exists predominantly in its cationic form (RhB^+) at pH 2.0. At pH 7.0, the fraction of RhB in positive form (RhB^+) decreases, while that in the zwitterion form (RhB^\pm) increases, which results in the decrease in RhB adsorption. In this condition, electrostatic repulsion or adsorption is not a determinative factor and the irradiation time determines the removal percentage of the RhB. The photocatalytic degradation percentage of RhB at a concentration of 5 mg.L^{-1} , an adsorbent dosage of 0.75 g.L^{-1} , and pH=7 was resulted 95.18 after 120 min. The pH_{PZC} of nano- Bi_2O_3 turned out to be 4.7, which is in agreement with the value reported in literature [25]. The surface charge of the catalyst becomes positive at pH lower than pH_{PZC} and reverse phenomenon takes place when pH is above pH_{PZC} . Furthermore, RhB adsorption decreased continuously at $pH \geq 7.0$, as the dominant speciation of RhB changed from being cationic to zwitterionic. This was mainly

due to the ionization of the carboxyl groups of RhB molecule, which was detrimental to RhB adsorption [26]. With increasing pH, deprotonation of the dye takes place, which hinders diffusion and a constant decrease in the amount of dye adsorbed is observed. In alkaline pHs, because of this electrostatic repulsion, the photocatalytic removal of RhB is low. Moreover, the hydroxyl groups on the surface of prepared catalysts act as an electron donor for photo-generated H^+ , and form active hydroxyl radicals ($\cdot\text{OH}$) which attack the dye [27,28], but there is a Coulombic repulsion between the negatively charged surface of photocatalyst and the hydroxide anions. This fact could prevent the formation of $\cdot\text{OH}$ and thus decreases the photooxidation [29]. This observation also indicated that it was very difficult to explain the effect of pH due to its multiple roles in affecting electrostatic interactions between the surfaces of catalysts and the reactants. Thus, a further detailed study is deemed necessary to clarify this matter.

Fig. 7b shows the surface and contour plots for the combined interaction of adsorbent dosage and irradiation time on the RhB degradation percentage. It can be concluded from the Fig. that RhB photo degradation increased with both catalyst dosage and irradiation time. This observation can be explained in terms of the availability of active sites on the catalyst surface. The combined interaction of X_1X_3 has a positive effect on RhB degradation as evidenced in Eq (4).

In order to investigate the combined interaction of irradiation time and RhB concentration (X_3X_4) on the response, the surface plot and contour plots of X_3X_4 interaction for degradation percentage were investigated (Fig 7(c)). It is evident from Fig 7(c) that the degradation percentage decreased with an increase of initial concentration that is attributed to the shielding effect. When the dye concentration exceeds the optimal amount, the dye reduces the penetration of the light in the solution, therefore decreases the photocatalytic yield [30]. On the other hand, an increase in catalyst dosage led to increase the RhB degradation. This means that the combined interaction of X_3X_4 has a negative impact on the response as revealed in the model (Eq.4).

3.6. Process optimization using response surface methodology

The last step of the RSM was to obtain the optimal conditions for the photocatalytic degradation of RhB over nano-photocatalyst (Bi_2O_3). An optimum condition for the RhB photocatalytic degradation process was the process that exhibits the maximum

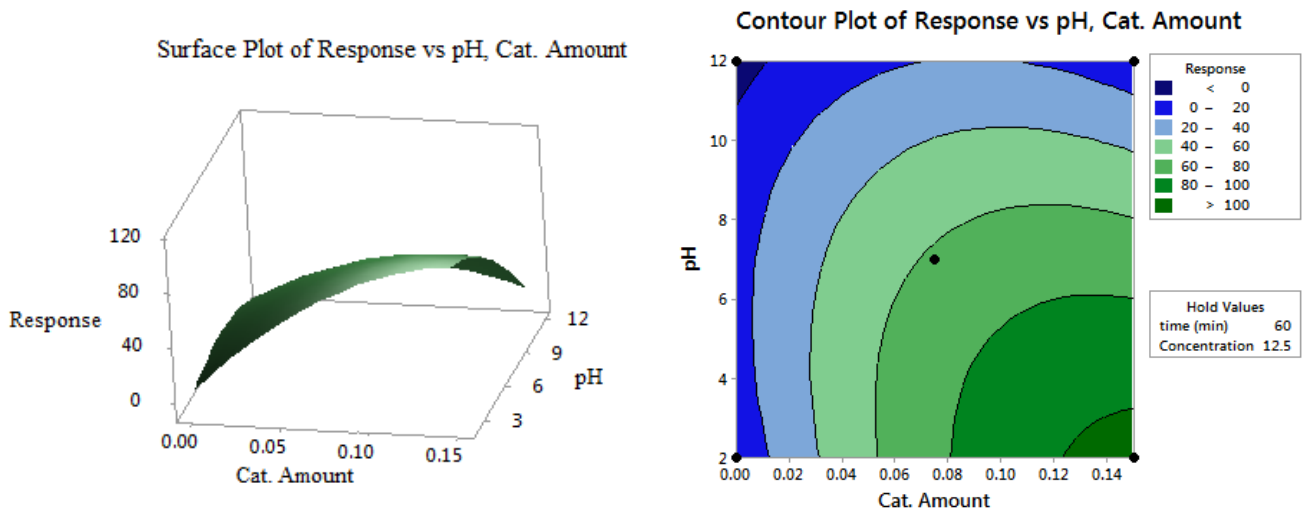


Fig. 7a. Response surface and contour-lines plots for catalyst amount and initial pH.

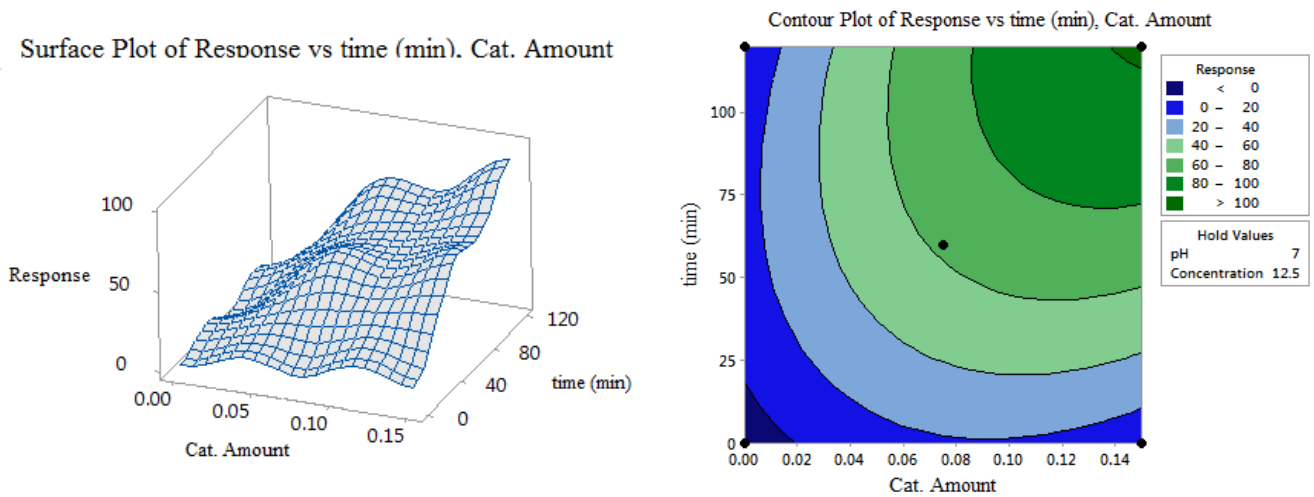


Fig. 7b. Response surface and contour-lines plots for catalyst amount and reaction time (min), holding the others variables at their center levels, initial pH 7 and initial concentration 12.5 ppm.

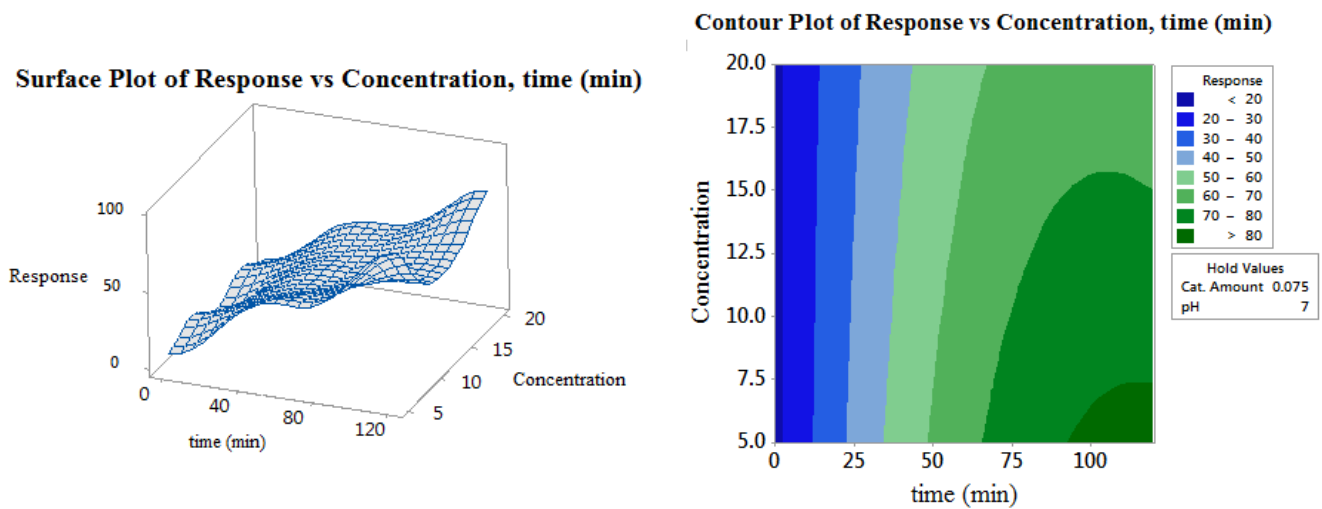


Fig. 7c. Response surface and contour-lines plots for concentration and reaction time (min).

RhB degradation at minimum catalyst dosage, optimal initial pH, irradiation time and high initial concentration of the RhB. The optimal conditions were found at catalyst dosage, initial pH irradiation time and initial concentration of 0.75 g.L⁻¹, 4.6 - 7, 120 min and 12.5 mg.L⁻¹ to achieve complete RhB degradation. The optimal experiment predicted by modeling was experimentally tested, in order to further assess the validity of the model. The response of experiment (RhB degradation) was 95%. Consequently, the validity and adequacy of the model were verified.

4. Conclusion

The nano-sized Bi₂O₃ was synthesized via a precipitation method and its photocatalytic activity was tested in degradation of Rhodamine B. The modeling of the process allowed to study the interaction of the binary factors and prediction of the degradation of Rhodamine B in different conditions. The relative importance of the independent factors of the process, suggested by Pareto analysis was as follows: Adsorbent dosage > initial pH ≈ irradiation time > dye concentration. Among binary terms of the model, interaction of adsorbent dosage- initial pH exhibited the prominent effect on the degradation of the dye. The results indicated that the photocatalytic degradation of RhB in acidic condition is much higher than in alkaline condition. The nano-Bi₂O₃ exhibited good photocatalytic activity in degradation of RhB under UV light.

Acknowledgements

The authors are grateful to Iran Nanotechnology Initiative Council for the financial support from this project.

References

- [1] L. Chen, S. Zhang, L. Wang, D. Xue, S. Yin, J. Crystal Growth. 311 (2009) 735-737.
- [2] R. Hu, C. Li, X. Wang, T. Zhou, X. Yang, G. Gao, Y. Zhang, Catal. Commun. 40 (2013) 71-75.
- [3] M. Su, C. He, V. Sharm, M. Abou Asi, D. Xia, X.Z. Li, H. Deng, Y. Xiong, J. Hazard. Mater. 211-212 (2012) 95-103.
- [4] J.L.X. Ding, H. Shu, J. Xie, H. Zhang, Mater. Sci. Eng. B 171 (2010) 31-34.
- [5] A. Nezamzadeh-Ejhi, Z. Banan, Iran. J. Catal. 2 (2012) 79-83.
- [6] L. Han, X. Zhou, L. Wan, Y. Deng, S. Zhan, J. Environ. Chem. Eng. 2 (2014) 123-130.
- [7] H. Faghihian, A. Bahrani, Iran. J. Catal. 1 (2011) 45-50.
- [8] C. Belver, C. Adan, M. Fernandez-Garcia, Catal. Today 143(2009) 274-281.
- [9] X. Liu, H. Cao, J. Yin, Nano Res. 4 (2011) 470-482.
- [10] T. Saison, N. Chemin, C. Chaneac, O. Durupthy, V. Ruaux, L. Mariey, F. Mauge, P. Beaunier, J.P. Jolivet, J. Phys. Chem. C 115 (2011) 5657-5666.
- [11] F. Qin, G. Li, R. Wang, J. Wu, H. Sun, R. Chen, Chem. Eur. J. 18 (2011) 16491-16497.
- [12] C. Pan, Y. Yan, H. Li, S. Hu, Adv. Mater. Res. 557-559 (2012) 615-618.
- [13] A.R. Khataee, M.B. Kasiriand, L. Alidokht, Environ. Technol. 32 (2011) 1669-1684.
- [14] S. Subramanian, J.S. Noh, J.A. Schwarz, J. Catal. 114 (1988) 433-439.
- [15] D. Salari, A. Niaei, F. Aghazadeh, S.A. Hosseini, F. Seyednajafi, J. Environ. Sci. Health A 47 (2012) 351-357.
- [16] A. Khuri, S. Mukhopadhyay, WIREs Comp. Stat. 2 (2010) 128-149.
- [17] L. Vafayi, S. Gharibe, Iran. J. Catal. 5 (2015) 365-371.
- [18] Z. Ai, Y. Huang, S. Lee, L. Zhang, J. Alloys Compd. 509 (2011) 2044-2049.
- [19] M.G. Ma, J.F. Zhu, R.C. Sun, Y.J. Zhu, Mater. Lett. 64 (2010) 1524-1527.
- [20] P. Tripathi, V.C. Srivastava, A. Kumar, Desalination 249 (2009) 1273-1279.
- [21] D. Wu, J. Zhou, Y. Li, Chem. Eng. Sci. 64 (2009) 198-206.
- [22] A.F. Shojaei, A.R. Tabari, M.H. Loghmani, Micro. Nano Lett. 8 (2013) 426-431.
- [23] R. Jaina, M. Mathura, S. Sikarwara, A. Mittal, J. Environ. Manage 85 (2007) 956-964.
- [24] S. Merouani, O. Hamdaoui, F. Saoudi, M. Chiha, Chem. Eng. J. 158 (2010) 550-557.
- [25] Y. Sun, W. Wang, L. Zhang, Z. Zhang, Chem. Eng. J. 211-212 (2012) 161-167.
- [26] Y. Gao, Y. Wang, H. Zhanga, Appl. Catal. B 178 (2015) 29-36.
- [27] H.R. Pouretdal, M. Ahmadi, Iran. J. Catal. 3 (2013) 149-155.
- [28] A. Nezamzadeh-Ejhi, M. Karimi-Shamsabadi, Chem. Eng. J. 228 (2013) 631-641.
- [29] U.G. Akpan, B.H. Hameed, J. Hazard. Mater. 170 (2009) 520-529.
- [30] M.H. Habibi, E. Askari, Iran. J. Catal. 1 (2011) 41-44.